Available online at www.sciencedirect.com
SCIENCE DIRECT®
International Journal of Thermal Sciences 42 (2003) 881–887
International Journal of Thermal Sciences
www.elsevier.com/locate/ijts

A parametric study on ice formation inside a spherical capsule

K.A.R. Ismail [a,*], J.R. Henríquez [b], T.M. da Silva [a]

[a] *Depto. de Engenharia Térmica e de Fluidos – FEM-UNICAMP CP: 6122, CEP 13083-970 Campinas, SP, Brazil*
[b] *Depto. de Engenharia Mecânica – DEMEC, UFPE, CEP 50740-530, Recife, PE, Brazil*

Received 27 August 2001; accepted 28 November 2002

Abstract

This paper reports the results of a numerical study on the heat transfer during the process of solidification of water inside a spherical capsule. The governing equations of the problem and associated boundary conditions were formulated and solved using a finite difference approach and a moving grid scheme. The model was optimized and the numerical predictions were validated by comparison with experimental results realized by the authors. The model was also used to investigate the effects of the size and material of the shell, initial temperature of the phase change material and the external temperature of the spherical capsule on the solidified mass fraction and the time for the complete solidification.

Keywords: Solidification in a spherical capsule; Moving boundaries; Phase-change heat transfer; Numerical simulation; Ice formation

1. Introduction

Industrial thermal processes of intermittent nature, or processes where energy availability and its utilization are not coincident require a means of matching the use of energy with its availability. This is usually done efficiently by energy storage system which stores energy when it is available and reutilize it when needed. Among the efficient ways of energy storage one can include the sensible and latent heat concepts. The latent heat concept is more attractive because of the large storage capacity and the constant charge and discharge temperatures. The PCM can be encapsulated in a variety of ways using cylindrical geometries with or without fins, cans, plates or spherical capsules. This last seems to offer a number of advantages which ranks it up among the most attractive methods of encapsulation. The spherical capsules are preferred due to favourable relation of volume of energy stored to the area for heat transfer and also because of easiness of packing into the storage tank with a good bed porosity.

Understanding the thermal behavior during phase change in spherical capsules is extremely important for the design of efficient storage systems.

Tao [1] presented a method for the analysis of solidification in cylindrical and spherical geometries. In the method proposed, an average heat transfer coefficient between the external surface of the solidified mass and the refrigerant was considered. He used a fixed grid approach to solve the mathematical model developed. Cho and Sunderland [2] used a transformation in the form of a product of radius times temperature and obtained a correction term to be applied to plane geometry to produce results adequate for spherical geometry. They presented good results for low Stefan number and at the initial stages of the solidification process.

Shih and Chou [3], proposed an iterative method of successive approximation to study the solidification process in spherical geometry. Their results showed good agreement when compared with numerical data available except for high values of Stefan number and low Biot number. Pedroso and Domoto [4] applied the perturbation technique to study the solidification process inside spheres of constant surface temperature and constant thermophysical properties. Riley et al. [5] realized an analytical study on the solidification inside cylinders and spheres for small Stefan numbers and constant thermal physical properties. They obtained series solutions which compared well with numerical results for Stefan number of 0.1.

* Corresponding author.
E-mail addresses: kamal@fem.unicamp.br (K.A.R. Ismail), rjorgeh@demec.ufpe.br (J.R. Henríquez).

1290-0729/$ – see front matter
doi:10.1016/S1290-0729(03)00060-7

Nomenclature

C	specific heat	$J\cdot kg^{-1}\cdot K^{-1}$
D	external shell diameter	
g	gravitational acceleration	$m\cdot s^{-2}$
$\bar{h}$	average convective heat transfer	$W\cdot m^{-2}\cdot K^{-1}$
k	thermal conductivity	$W\cdot m^{-1}\cdot K^{-1}$
L	latent heat of fusion	$J\cdot kg^{-1}$
m^*	solidified mass fraction	
M_{Solid}	solidified mass	kg
M_{Total}	total mass	kg
n_l, n_s	number of intervals in the liquid and solid region	
$\overline{Nu}_D$	average Nusselt number, $= \frac{\bar{h}D}{k}$	
Pr	Prandtl number, $= \frac{\nu}{\alpha}$	
r	radial coordinate	m
Ra_D	Rayleigh number, $= \frac{g\beta(T_w - T_0)D^3}{\alpha\nu}$	
R_e	external shell radius	m
R_i	internal shell radius	m
$S(t)$	interface position	m
t	time	s
T	temperature	K
T_0	refrigerant temperature	K
T_{PC}	phase change temperature	K

Greek symbols

α	thermal diffusivity, $= k/(\rho C)$	$m^2\cdot s^{-1}$
β	volumetric thermal expansion coefficient	K^{-1}
μ	viscosity	$kg\cdot s^{-1}\cdot m^{-1}$
ν	kinematic viscosity	$m^2\cdot s^{-1}$
ρ	density	$kg\cdot m^{-3}$

Subscripts

c	capsule
e	external
i	internal
j	position of the grid
l	liquid phase
PC	phase change
s	solid phase
w	wall

Moore and Bayazitoglu [6] studied the melting process of PCM within a spherical enclosure. The phase change material is initially considered at its saturation temperature. Suddenly the enclosure temperature is increased and consequently the melting process starts. Assuming that the solid density is more than the liquid density, the solid continually drops towards the bottom of the shell as melting progresses. A mathematical model is developed and the interface positions and the temperature profiles for various Stefan and Fourier numbers are determined and the energy storage characteristics are studied.

Hill and Kucera [7] developed a new semi-analytical procedure to study the solidification inside a spherical container including the effects of radiation at the container surface. The numerical values obtained for the position of the moving front are in agreement with available results from a completely numerical solution and an alternative semi-analytical solution of the problem. Milanez [8] and Milanez and Ismail [9] presented a moving grid numerical solution of the PCM solidification in spherical geometry and compared their results with approximate models and also with experiments. Prud'homme et al. [10] applied the method of strained coordinates to study the inward solidification in slabs, cylinders and spheres. The unified approach adopted allows the simultaneous treatment of the problem in plane, cylindrical and spherical geometries for three different types of boundary conditions. A general recurrence formula is derived for the determination of the series solutions up to any desired order of Stefan number.

Cho and Choi [11] investigated experimentally the thermal behavior of paraffin inside a spherical capsule during solidification and fusion, compared the results with that of water as a PCM and found that water presented more supercooling than paraffin. In another work on the solidification of water inside cylindrical capsules Chen et al. [12] demonstrated that for lower refrigerant temperatures the probability of nucleation is more probable. They also studied the effect of capsule size to reduce the supercooling and found that large capsules indicate increase in the nucleation. Additionally two relevant papers by Bedecarrats et al. [13] and Dumas et al. [14] investigated the process of energy storage in a tank full with spherical capsules. In these studies they presented a mathematical model for the melting and solidification of the PCM in the spherical capsules and a simplified model for the charging and discharging of the storage tank. The proposed model includes a probabilistic study of the super cooling phenomenon in the spherical capsules as in Bedecorrats and Dumas [15]. Experimental results for water as a PCM are presented in [13–15].

A recent published book by Ismail [16] on cold storage systems, fundamentals and modeling treated the formulation and analysis of ice storage systems using spherical capsules and other geometries. Many research work and results related to the area are presented and discussed.

This paper presents a model and its numerical solution based upon the finite difference approximations for the solidification of PCM in a spherical container under convective boundary conditions at the external surface of the spherical shell. Important parameters such as size of the spherical capsule, wall material, external temperature and the initial PCM temperature are investigated and their effects on the solidified mass fraction and the time for complete solidification were presented and discussed.

2. Formulation

Consider a spherical shell of external radius R_e initially filled with liquid PCM at an arbitrary initial temperature higher than the phase change temperature T_{PC}. Suddenly at $t = 0$, the spherical shell is subject to convective cooling in a thermal bath maintained at a constant temperature $T = T_0$, lower than the phase change temperature. Sensible heat exchange takes place initially and causes the cooling of the liquid contained into the spherical shell until the layer in contact with the spherical surface reaches the phase change temperature and consequently forms the first solidified layer considering that the proposed model does not include the supercooling phenomenon. From this moment on, the process of continuous phase change occurs until all the liquid is solidified. Starting from this stage, a pure conductive cooling occurs in the solid until the system reaches thermal equilibrium with the constant temperature thermal bath.

During the initial and final stages, that is, pure liquid and complete solid, the heat transfer process is represented by a pure conduction model. In case of the two phases coexisting, the process is modeled by a conduction model with phase change. The convective effects present in the liquid region of the PCM are accounted for by using the concept of effective thermal conductivity coefficient in the energy equation. This coefficient is initially evaluated by comparing the heat exchange by convection with the heat which could be exchanged by pure conduction. For the case of convection, the correlation of Hutchins and Marschall [17] was used while the equivalent thermal conductivity coefficient was determined from Holman [18]. For the case of sphere of diameter of 0.12 m, wall temperature of 0 °C and internal fluid temperature of 20 °C, the estimated effective thermal conductivity coefficient based on Hutchins and Marschall [17] correlation is found to be $k_{eff} = 8.2\ \mathrm{W{\cdot}m^{-1}{\cdot}K^{-1}}$ while the value calculated from Holman [18] is found to be $k_{eff} = 1.4\ \mathrm{W{\cdot}m^{-1}{\cdot}K^{-1}}$. The two values are considered as initial limiting estimates for the effective thermal conductivity and the final value adopted was determined by adjustments based on experimental results. The value of $k_{eff} = 2.5\ \mathrm{W{\cdot}m^{-1}{\cdot}K^{-1}}$, for the thermal conductivity of the liquid phase k_l, used in the numerical simulations resulted in better agreement with the experimental results as shown in Figs. 1 and 2.

In the first and third stages a conduction model is considered in the liquid (b = l) and solid (b = s) phases, respectively, and the corresponding governing equations and the boundary conditions can be written as

$$\frac{\partial T_b}{\partial t} = \left(\frac{k}{\rho C}\right)_b \left[\frac{2}{r}\frac{\partial T_b}{\partial r} + \frac{\partial^2 T_b}{\partial r^2}\right] \quad 0 < r < R_i \tag{1}$$

$$-k_b \frac{\partial T_b}{\partial r} = (T_b - T_0)\left\{\frac{(R_e - R_i)}{k_c}\left(\frac{R_i}{R_e}\right) + \left(\frac{R_i}{R_e}\right)^2 \frac{1}{\bar{h}}\right\}^{-1} \quad r = R_i \tag{2}$$

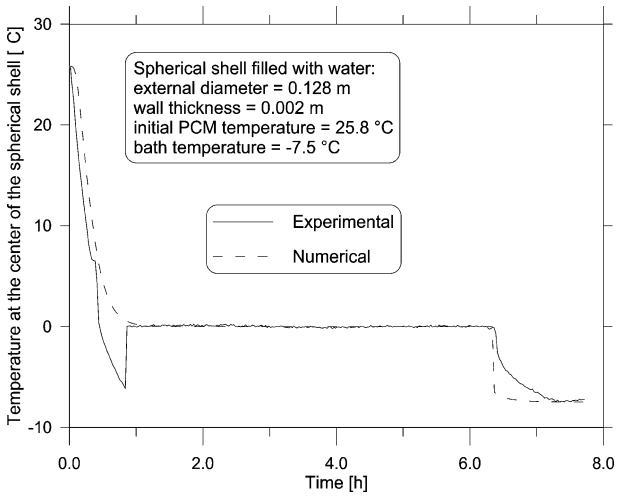

Fig. 1. Variation of the temperature at the center of the sphere with time for bath temperature of −7.5 °C.

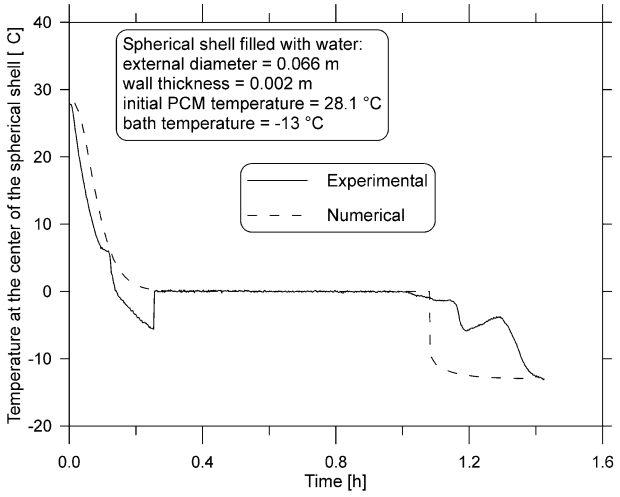

Fig. 2. Variation of the temperature at the center of the sphere with time for bath temperature of −13 °C.

$$\frac{\partial T_b}{\partial r} = 0, \quad r = 0 \tag{3}$$

The second stage when the PCM is changing phase the corresponding model can be written in the form

Solid region

$$\frac{\partial T_s}{\partial t} = \left(\frac{k_s}{\rho_s C_s}\right)\left[\frac{2}{r}\frac{\partial T_s}{\partial r} + \frac{\partial^2 T_s}{\partial r^2}\right], \quad S(t) < r < R_i \tag{4}$$

Liquid region

$$\frac{\partial T_l}{\partial t} = \left(\frac{k_l}{\rho_l C_l}\right)\left[\frac{2}{r}\frac{\partial T_l}{\partial r} + \frac{\partial^2 T_l}{\partial r^2}\right], \quad 0 < r < S(t) \tag{5}$$

$$-k_s \frac{\partial T_s}{\partial r} = (T_s - T_0) \times \left\{\frac{(R_e - R_i)}{k_c}\left(\frac{R_i}{R_e}\right) + \left(\frac{R_i}{R_e}\right)^2 \frac{1}{\bar{h}}\right\}^{-1} \quad r = R_i \tag{6}$$

$$\frac{\partial T_l}{\partial r} = 0, \quad r = 0 \tag{7}$$

$$T_s = T_l = T_{PC}, \quad r = S(t) \tag{8}$$

$$k_s \frac{\partial T_s}{\partial r} - k_l \frac{\partial T_l}{\partial r} = \rho L \frac{dS(t)}{dt}, \quad r = S(t) \tag{9}$$

$k_l = k_{eff}$ in the model equations.

The convection heat transfer condition at the external surface of the spherical shell can be treated by using the mean Nusselt number given as

$$\overline{Nu}_D = \frac{\bar{h} D}{k} \tag{10}$$

If the spherical shell is immersed in a stagnant fluid whose temperature is different from that of the spherical shell surface, natural convection currents are produced and the convective mean heat transfer coefficient can be obtained by using Churchill [19]

$$\overline{Nu}_D = 2 + \frac{0.589 Ra_D^{1/4}}{[1 + (0.469/Pr)^{9/16}]^{4/9}} \tag{11}$$

where $Ra_D = \frac{g\beta(T_w - T_0)D^3}{\alpha\nu}$, T_w is the temperature of the external surface of the shell and T_0 is the temperature of the stagnant fluid Using this correlation it is possible to correct continually the heat transfer coefficient as the surface temperature of the spherical capsule changes during the process of cooling and phase change. In other words, the model takes into account the changes in the natural convection intensity on the external surface of the capsules.

3. Numerical solution

The model presented by Eqs. (1)–(9), was solved numerically by the use of an implicit finite difference approach and a moving grid scheme based on the technique used by Murray and Landis [20] for plane geometry and also by Milanez and Ismail [9] for the case of spherical geometry. This scheme is chosen because of its numerical simplicity in treating moving fronts as shown in Fig. 3. Using this method the interface position will always coincide with a discrete mesh node which facilitates the localization of the interface during the solidification process. To implement the moving grid method, the problem domain is divided into two regions, solid and liquid separated by the interface. The solid region $[S(t) \leqslant r \leqslant R_1]$ is divided into n_s equal increments of size Δr_s. During the process of phase change the solidification front moves continually towards the center of the sphere and consequently extends the grid defined for the solid region and increases the grid size Δr_s. Opposite effects are found in the region defined for the liquid phase $[0 \leqslant r \leqslant S(t)]$, which is subdivided into n_l equal increments Δr_l. The method of Murray and Landis [20] allows modifying Eqs. (4) and (5), in such a way to allow for expansion and contraction of the solid and liquid regions. This is done by considering the total derivative of the temperature in the solid and in the liquid domains as given by equation

$$\frac{DT_b}{Dt} = \frac{\partial T_b}{\partial r}\frac{dr}{dt} + \frac{\partial T_b}{\partial t} \tag{12}$$

According to Fig. 3, the position of arbitrary points inside the grid in the solid and liquid regions is given by

$$r_{s_j} = (j-1)\frac{[R_i - S(t)]}{n_s} + S(t) \tag{13a}$$

$$r_{l_j} = (j-1)\frac{S(t)}{n_l} \tag{13b}$$

The change in position of the points r_{sj} and r_{lj} due to the to the change in the grid size can be written as

$$\frac{dr_{s_j}}{dt} = \frac{dS(t)}{dt} - \frac{(j-1)}{n_s}\frac{dS(t)}{dt} \tag{14a}$$

$$\frac{dr_{l_j}}{dt} = \frac{(j-1)}{n_l}\frac{dS(t)}{dt} \tag{14b}$$

Substituting Eqs. (12) and (14) into Eqs. (4) and (5), one can obtain the modified heat conduction equations. These equations are valid for a discrete domain and include time variation of the grid in the liquid and solid regions

$$\frac{dT_l}{dt} = \left[\frac{2}{r}\left(\frac{k_l}{\rho_l C_l}\right) + \frac{r}{S(t)}\frac{dS(t)}{dt}\right]\frac{\partial T_l}{\partial r} + \left(\frac{k_l}{\rho_l C_l}\right)\frac{\partial^2 T_l}{\partial r^2} \tag{15}$$

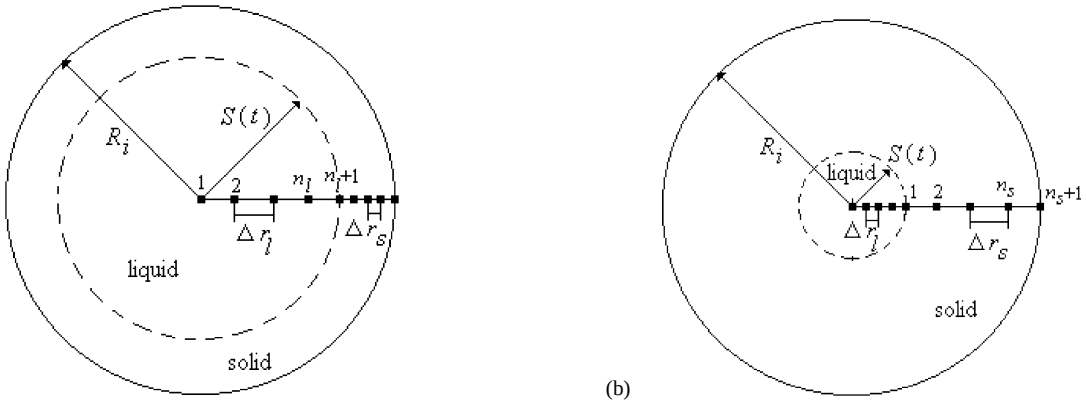

Fig. 3. Interface position and the computational grid for two time instants; (a) time t, (b) time $t + \Delta t$.

$$\frac{dT_s}{dt} = \left[\frac{2}{r}\left(\frac{k_s}{\rho_s C_s}\right) + \frac{R_i - r}{R_i - S(t)}\frac{dS(t)}{dt}\right]\frac{\partial T_s}{\partial r} + \left(\frac{k_s}{\rho_s C_s}\right)\frac{\partial^2 T_s}{\partial r^2} \quad (16)$$

With the above modifications implemented in the heat conduction equation, Eqs. (15) and (16) replace Eqs. (4) and (5) in the mathematical model. The resulting system of equations written in implicit finite difference form is valid for all points in the domain. This procedure results in a system of algebraic equations which is solved simultaneously. When the PCM is completely solid or completely liquid, a fixed grid method can be used to discretize the corresponding equations.

Numerical tests were realized to optimize the numerical calculations and render the results free of the grid size. The results indicated that 40 radial points (20 points in the liquid region and another 20 points in the solid region) and time interval (Δt) of 0.1 s are satisfactory and consequently these values were used in all the numerical simulations.

4. Results and discussion

Although this work is not supposed to be experimental, some experimental measurements were realized to validate the proposed model using water as the PCM. The experimental rig is composed of spherical capsules of Pyrex glass of different diameters filled with phase charge material. The spherical shell is placed in a constant temperature Ethanol bath fitted with control system to register and maintain the temperature of the bath constant. The bath is in the form of a tank of $0.08 \times 0.08 \times 0.07$ m, sufficiently big volume to minimize the variations of temperature during the heat exchange process between the Ethanol and the spherical capsule. The temperature of the bath is controlled within $\pm 0.1\,^{\circ}$C. In the experimental procedure the spherical capsule is filled with water at temperature between 25 °C and 30 °C and is submersed into the Ethanol thermal bath maintained at constant temperature below 0 °C. Thermocouples placed at the center of the spherical capsule, and on the outer and inner surfaces of the shell are used to register the temperature during the cooling and solidification of water in the shell. The experiment is terminated when the PCM at the center of the shell reaches 0 °C and thermal equilibrium is achieved between the bath and the spherical shell.

Table 1
Experimental parameters

Capsule:	Pyrex glass (0.002 m wall thickness)	
PCM	Water	
Bath	Ethanol	
	Case 1	Case 2
External diameter (m):	0.128	0.066
Bath temperature (°C):	−7.5	−13
Initial PCM temperature (°C):	25.8	28.1

Figs. 1 and 2 show comparative results of the numerical predictions from the present model and experimental tests realized to validate the model under the same geometrical and operational conditions. Table 1 shows the experimental conditions used in the experiments while Table 2 shows the thermo physical properties used in the numerical simulations.

The experimental curves indicate a degree of supercooling, which is not possible to be predicted by the present model. According to Chen et al. [12], the degree of supercooling depend upon the temperature of the external fluid and the size of the capsule. The addition of nucleating agents to the PCM helps to reduce supercooling. Although it was mentioned that the proposed model is unable to reproduce the supercooling phenomenon and that the numerical predictions indicated higher cooling rate after complete solidification, one can observe a relatively good agreement between the experiments and the numerical predictions. The authors attribute the differences between the numerical and experimental results after terminating the solidification process to purely numerical effects caused by false numerical diffusion. Different numerical tests were tried to eliminate this difference without great success. Considering that the sensible heat stored in this stage of the process is very small in comparison with the total heat stored (sensible and latent), one can admit that the results are valid without big errors.

Having validated the model and numerical results, the model is used to study the influence of the size and material of the capsule shell, initial temperature of the phase change material and the external temperature of the spherical capsule on the solidified mass fraction and the time for the complete solidification.

Adopting that the densities of the liquid and solid phases of the PCM are equal, the solidified mass fraction is defined as

$$m^* = \frac{M_{Solid}}{M_{Total}} = 1 - \left[\frac{S(t)}{R_i}\right]^3 \quad (17)$$

The effect of the material of the spherical capsule on the solidified mass fraction is shown in Fig. 4. The materials tested are cupper, aluminium, polyethylene, acrylic and PVC. This effect is included in the model as a thermal resistence due to the wall effect of the capsule and is indicated in Eqs. (2)

Table 2
Thermophysical properties

PCM: Liquid	Solid
$k_l = 0.56$ (W·m^{-1}·K^{-1})	$k_s = 2.21$ (W·m^{-1}·K^{-1})
$\alpha_l = 1.34 \times 10^{-7}$ (m^2·s^{-1})	$\alpha_s = 1.18 \times 10^{-6}$ (m^2·s^{-1})
$C_l = 4210$ (J·kg^{-1}·K^{-1})	$C_s = 4210$ (J·kg^{-1}·K^{-1})
$L = 333.4 \times 10^{-3}$ (J·kg^{-1})	

Capsule material:

Pyrex Glass: $k = 1.4$ (W·m^{-1}·K^{-1})	Polyethylene: $k = 0.35$ (W·m^{-1}·K^{-1})
Cupper: $k = 372$ (W·m^{-1}·K^{-1})	Acrylic: $k = 0.15$ (W·m^{-1}·K^{-1})
Aluminium: $k = 204$ (W·m^{-1}·K^{-1})	PVC: $k = 0.18$ (W·m^{-1}·K^{-1})

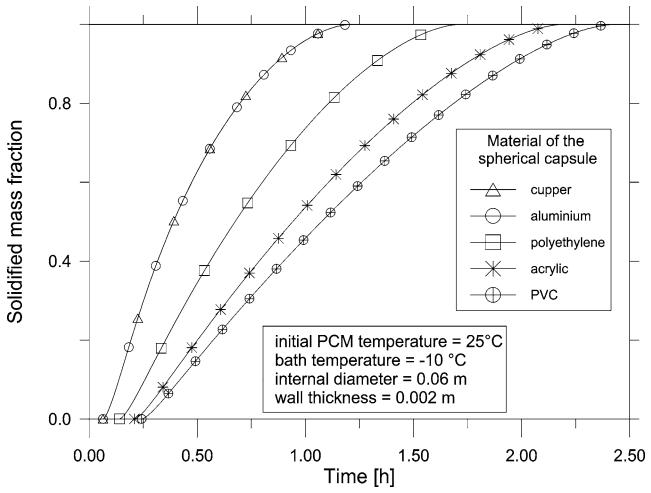

Fig. 4. Effect of the material of the spherical capsule on the solidified mass fraction.

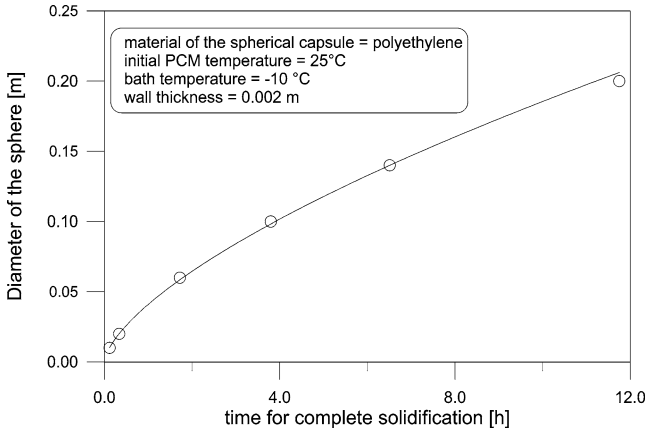

Fig. 5. Effect of the sphere size on the time for complete solidification.

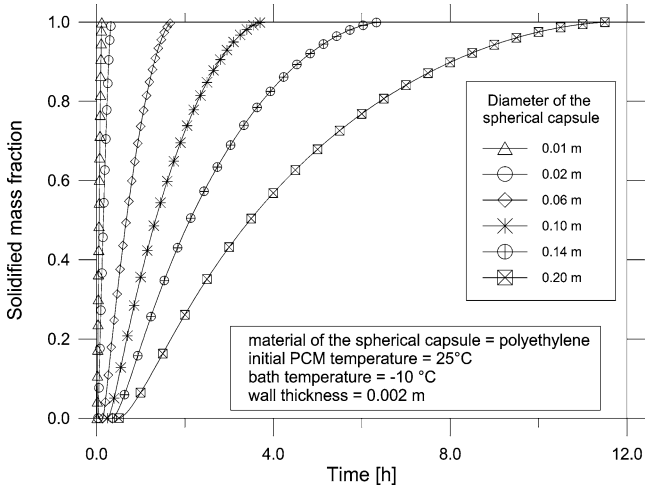

Fig. 6. Effect of the sphere size on solidified mass fraction.

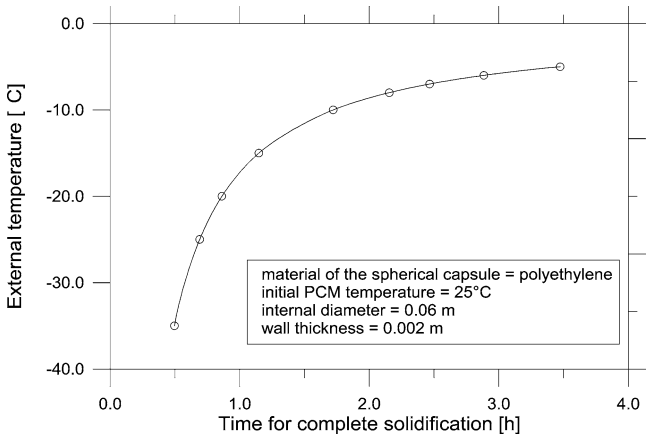

Fig. 7. Effect of the external fluid temperature on the time for complete solidification.

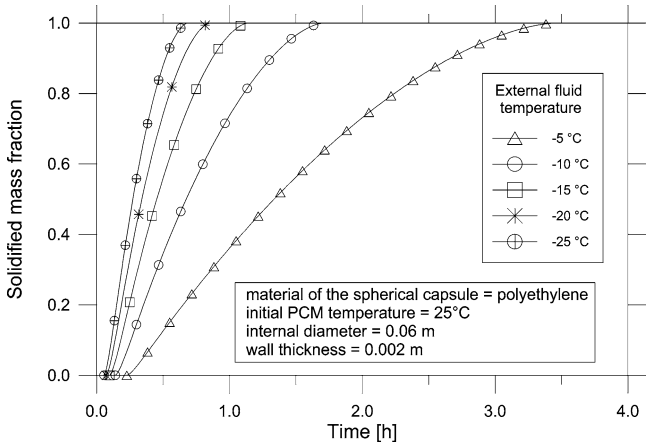

Fig. 8. Effect of the external fluid temperature on the solidified mass fraction.

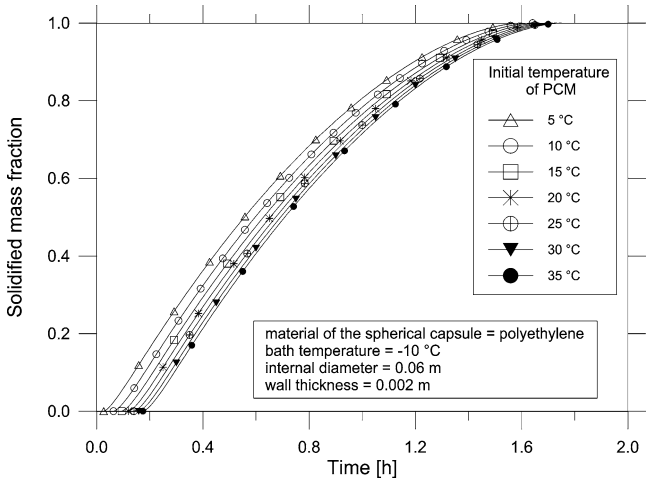

Fig. 9. Effect of the initial temperature on the time for complete solidification.

and (6). In the case of the metallic materials, the solidification curves are coincident. Comparison with the results of the polyethylene, acrylic and PVC, indicate that the polyethylene is found to exhibit better performance than acrylic and PVC It is interesting to notice the difference between the times for complete solidification in the case of metalic and nonmetalic spherical shells. This difference of around 30 minutes makes the use of the nonmetalic capsules very attractive.The effect of the capsule size is also studied by realizing numerical simulation on spherical shells of different diameters and constant wall thickness of 2 mm. The initial temperature of the PCM is 25 °C and the thermal bath temperature of −10 °C. As expected big spherical shells takes more time to solidify completely than smaller shells as shown in Fig. 5.

One can observe from Figs. 5 and 6 that a sphere of 0.1 m in diameter takes about four hours to solidify completely while a sphere of 0.2 m diameter takes about 12 hours.

Figs. 7 and 8 present the effect of the temperature of the working fluid on the time for complete solidification and the solidified mass fraction. The temperature of the working fluid was varied from −5 °C to −25 °C while keeping the other parameters unchanged. As can be seen from Fig. 7, the decrease of the working fluid temperature from −5 °C to −15 °C reduced greatly the time for complete phase change. More reduction of the working fluid temperature did not lead to corresponding reduction in the time for complete phase change. One can observe from Fig. 8 that as the temperature of the external fluid is reduced the curves of solidified mass fraction seem to be closer together. Finally to study the effect of the initial temperature of the PCM on the time for complete solidification and the solidified mass fraction, the initial temperature of the PCM was varied from 5 to 35 °C while keeping the rest of parameters unchanged. The results shown in Fig. 9 demonstrate that this influence is marginal. Fig. 9 shows the time for complete solidification (the solidified mass fraction equals to unity), nearly equal for all initial temperatures indicating the small effect of the initial temperature of the PCM.

5. Conclusions

The numerical results validated with experimental measurements indicate that the proposed model for internal spherical solidification is adequate and the numerical predictions are consistent and compare well with available results. One can verify that the time for complete solidification increases with the increase of the size of the spherical shell and with the increase of the external fluid temperature.

As mentioned the thermal conductivity of the capsule material has a strong effect on the time for complete solidification and the solidified mass fraction. Although metalic material has higher thermal conductivity than other nonmetalic material such as Polyethylene, the reduction in the time for complete solidification is around 30 minutes and consequently justifies the use of nonmetalic capsules.

Acknowledgements

The authors wish to thank the CNPq (Conselho Nacional de Desenvolvimento Científico e Tecnológico) for the scholarships to the authors and the financial support for the integrated project. The authors also wish to thank Esferas Douglas Limited for offering the plastic spheres.

References

[1] L.C. Tao, Generalized numerical solutions of freezing a saturated liquid in cylinders and spheres, AIChE J. 13 (1967) 165–169.
[2] S.H. Cho, J.E. Sunderland, Phase change of spherical bodies, Internat. J. Heat Mass Transfer 13 (1970) 1231–1233.
[3] Y.P. Shih, T.C. Chou, Analytical solution for freezing a saturated liquid inside or outside spheres, Chem. Engrg. Sci. 26 (1971) 1787–1793.
[4] R.I. Pedroso, G.A. Domoto, Perturbation solutions for spherical solidification of saturated liquids, J. Heat Transfer 95 (1973) 42–46.
[5] D.S. Riley, S.T. Smith, G. Poots, The inward solidification of spheres and circular cylinders, Internat. J. Heat Mass Transfer 17 (1974) 1507–1516.
[6] F.E. Moore, Y. Bayazitoglu, Melting within a spherical enclosure, J. Heat Transfer 104 (1982) 19–23.
[7] J.M. Hill, A. Kucera, Freezing a saturated liquid inside a sphere, Internat. J. Heat Mass Transfer 26 (1983) 1631–1637.
[8] L.F. Milanez, Desenvolvimento teórico e verificação experimental de modelos para a solidificação em geometria esférica, Doctor Thesis, Faculdade de Engenharia Mecânica, UNICAMP, Campinas, SP, Brasil, 1984.
[9] L.F. Milanez, K.A.R. Ismail, Solidification in spheres, theoretical and experimental investigation, in: 3th International Conference on Multi-Phase and Heat Transfer, Miami, 1984.
[10] M. Prud'homme, T.H. Nguyen, D.L. Nguyen, A heat transfer analysis for solidification of slabs, cylinders, and spheres, J. Heat Transfer 111 (1989) 699–705.
[11] K. Cho, S.H. Choi, Thermal characteristics of paraffin in a spherical capsule during freezing and melting processes, Internat. J. Heat Mass Transfer 43 (2000) 3183–3196.
[12] S.L. Chen, P.P. Wang, T.S. Lee, An experimental investigation of nucleation probability of supercooled water inside cylindrical capsules, Experimental Thermal Fluid Sci. 18 (1999) 299–306.
[13] J.P. Bedecarrats, F. Strub, B. Falcon, J.P. Dumas, Phase change thermal energy storage using spherical capsules: Performance of a test plant, Internat. J. Refrig. 19 (3) (1996) 187–196.
[14] J.P. Dumas, J.P. Bedecarrats, F. Strub, B. Falcon, Modelization of a tank filled with spherical nodules containing a phase change material, in: Proceeding 10th International Heat Transfer Conference Brighton, August 1994, Vol. 7, pp. 239–244.
[15] J.P. Bedecarrats, J.P. Dumas, Étude de la cristallisation de nodules contenant un materiau à changement de phase en vue du stockage par chaleur latente, Internat. J. Heat Mass Transfer 40 (1) (1997) 149–157.
[16] K.A.R. Ismail, Bancos de Gelo: Fundamentos e Modelagem, Editora e Gráfica Imagem, Campinas, SP, 1998, ISBN 85-900609-2-6, 400 p.
[17] J. Hutchins, E. Marschall, Pseudosteady-state natural convection heat transfer inside spheres, Internat. J. Heat Mass Transfer 32 (1989) 2047–2053.
[18] J.P. Holman, Transferência de Calor, McGraw-Hill do Brasil, São Paulo, 1983.
[19] S.W. Churchill, Free convection around immersed bodies, in: E.U. Schlünder (Ed.), Heat Exchanger Design Handbook, Hemisphere, New York, 1983, Section 2.5.7.
[20] W.D. Murray, F. Landis, Numerical and machine solution of transient heat-conduction problems involving melting or freezing, Internat. J. Heat Transfer (1959) 108–112.